


Research Article

Effect of Detuning of Clamping Force of Tie Rods on Dynamic Performance of Rod-Fastened Jeffcott Rotor

Haoliang Xu,^{1,2,3} Lihua Yang ,^{1,2,3} Tengfei Xu,^{1,2,3} and Yao Wu^{1,2,3}

¹State Key Laboratory for Strength and Vibration of Mechanical Structures, Xi'an Jiaotong University, Xi'an 710049, Shaanxi, China

²Shaanxi Key Laboratory of Environment and Control for Flight Vehicle, Xi'an Jiaotong University, Xi'an 710049, Shaanxi, China

³School of Aerospace Engineering, Xi'an Jiaotong University, Xi'an 710049, Shaanxi, China

Correspondence should be addressed to Lihua Yang; yanglihua_2@126.com

Received 29 October 2020; Revised 17 December 2020; Accepted 7 January 2021; Published 16 January 2021

Academic Editor: Adrian Neagu

Copyright © 2021 Haoliang Xu et al. This is an open access article distributed under the Creative Commons Attribution License, which permits unrestricted use, distribution, and reproduction in any medium, provided the original work is properly cited.

In view of the advantages of lightweight, high strength, easy cooling, and easy assembly, the rod-fastened rotor is widely used in the aeroengine and heavy gas turbine. However, because of assembly, stress relaxation, material creep, and other reasons, the clamping force of the tie rods will be out of tune during the long-term operation of the rotor. The detuning of the clamping force of the tie rods not only affects the contact stiffness of the contact interface but also causes the rod-fastened rotor with a certain residual shaft bow, which will affect the dynamic characteristics of the rod-fastened rotor. Based on the statistical model of rough surface contact (GW contact model), this paper presents a method to calculate the equivalent flexural stiffness of rough surface considering the detuning of the clamping force of the tie rods and gives the calculation method of the residual shaft bow deformation of the rod-fastened Jeffcott rotor with detuning of the tie rods. The effect of the preload, the rate of detuning of the tie rods, the number of detuning tie rods on the natural frequency, and the response of residual shaft bow of the rod-fastened Jeffcott rotor at a certain speed are investigated. The results show that the detuning of the tie rods makes the flexural stiffness of the rotor inconsistent along with two main stiffness directions of the rotor, which makes the natural frequency of the rotor divided into two. The negative detuning of the tie rods decreases the natural frequency of the rotor, while the positive detuning of the tie rods increases the natural frequency of the rotor. The smaller preload or the larger rate of detuning of the tie rods makes the detuning of the tie rods have a greater influence on the natural frequency of the rotor. These results will provide a theoretical reference for the dynamic analysis and design of the rod-fastened rotor.

1. Introduction

The rod-fastened rotor is a kind of rotor structure widely used in aeroengine and gas turbines. It depends on one central tie rod or several circumferential tie rods to clamping the discs together. The rod-fastened rotor is a typical assembled structure, which has the advantages of lightweight, easy cooling, convenient assembly, and flexible selection of disc material. However, the complex structure also brings some difficulties in the dynamic analysis. The contact states of the interfaces between the discs are mainly ensured by the clamping force from the tie rods. Therefore, the clamping force is crucial, which will directly affect the contact stiffness of the contact interfaces of the discs. In the process of

assembling, the tie rods are elongated to offer the preload to the discs. However, because of assembling, stress relaxation, and material creep, the clamping force of the tie rods will be uneven, which results in the detuning of the clamping force along the circumferential direction in the contact surfaces. It will affect the flexural stiffness of the rotor shaft segment and the dynamic performances. Besides, the detuning of the clamping force of the tie rods leads to the rotor with a residual shaft bow, which affects the amplitude of the rotor system. Some faults of the rotor system are from serious vibration. So the research on the effect of the detuning of clamping force on the dynamic characteristics of the rod-fastened rotor is quite necessary. However, few investigations have been focused on this aspect.

In recent years, some scholars put forward the dynamic model of the rod-fastened and analyze the dynamic behavior of it. Rao [1] built a mechanic model of the rod-fastening rotor based on a comprehensive analysis of the structural characteristics of the rod-fastened rotor. The correctness of the model is proved by comparing it with experimental results. Qi et al. [2] studied the dynamic characteristics of the gas turbine rotor considering contact effects and pretightening forces. An improved 2-D FEM method considering the contact effect was given and improved the computing accuracy of the critical speed of the rotor. Zhang et al. [3] provided a determination method of contact stiffness based on the modal test and finite element analysis, which was proven to be effective. Jam et al. [4] proposed a finite element model for vibration analysis of rod-fastened rotor. The results proved that the finite element model is effective. Peng et al. [5–7] studied the overall contact behavior between an elastic-plastic hemisphere and a rigid plane and the elastic-plastic contact between two rough statistical surfaces. Then, a dynamic analysis of a rod-fastened rotor based on elastic-plastic contact was investigated. Lu et al. [8] investigated the dynamic characteristic of the gas turbine rotor considering contact effect and tie rods by the finite element method. Gao et al. [9] investigated the effects of bending moments and pretightening forces on the flexural stiffness of contact interfaces in rod-fastened rotors. Liu Heng et al. [10, 11], Yuan et al. [12], and Hu et al. [13] investigated the non-linear dynamic behaviors of the circumferential rod-fastened rotor. These studies show that the preload is a crucial parameter to determine the contact stiffness of the interfaces between discs, which affects the dynamic behavior of the rotor system. Besides, some investigations focused on the dynamic performances of the rotor with residual shaft bow. Nicholas et al. [14] studied the influence of residual shaft bow on unbalance response of a simple rotor by theoretical analysis, and three ways to balance a rotor with residual shaft bow were given. Flack et al. [15] conducted a theoretical and experimental comparison of unbalance responses of a bowed Jeffcott rotor supported by five different sets of fluid film bearings. A transfer matrix method was used to calculate the vibration response of the rotor system. Shiau et al. [16] investigated the effects of residual shaft bow on dynamic performances of a simply supported rotor with mass unbalances and disk skew, and the effect of disk positioning between supports was also discussed. From the point of fault diagnosis, Rao [17] discussed the vibration problem of the Jeffcott model with a residual bow during its operation time. Several observations were proposed to identify the presence of a rotor with the bow. Kang et al. [18] studied the dynamic characteristics of a geared rotor-bearing system in which the residual shaft bow, the gear eccentricity, and the gear's transmission error were considered. Song et al. [19] studied the vibration of a rotor with a residual shaft bow by simulation and experiment. Sanches et al. [20] discussed how to identify the two most common faults of unbalance and residual shaft bow in rotating machines by theoretical and experimental techniques.

The above reports are all focused on the normal rotors, which have no detuning of the clamping force of the tie rods. However, in engineering, the uneven clamping force is unavoidable because of the assembling, self-loosening of the bolt, and material creep. Therefore, this paper investigates the dynamic performances of the rod-fastened rotor with the uneven clamping force of the tie rods. First, based on the GW contact model (the statistical model of rough surface contact proposed by Greenwood and Williamson), a method of calculation of the flexural stiffness of the interfaces with the detuning of the clamping force of the tie rods is proposed. Meanwhile, residual shaft bow deformation of the rotor resulted from the detuning of the clamping force of the tie rods is given. Then, the effect of preload, the rate of the detuning of the tie rods, and the number of the detuning tie rods on the dynamic performance of the rotor system are investigated. Some useful conclusions will provide a reference to the dynamic design of the rod-fastened rotor.

2. Theoretical Analysis

2.1. The Flexural Stiffness of the Rod-Fastened Jeffcott Rotor.

The rod-fastened Jeffcott rotor depends on the eight circumferential tie rods to clamping the two shaft heads, and there is an annular contact interface between the two shaft heads (see Figure 1). The length of both end shaft segments is L_1 , respectively. The length of the clamped shaft segment is L_2 . The elastic modulus of the material is E . The moment of inertia of the end shaft segments is I_1 , and the moment of inertia of the clamped shaft segment is I_2 . Due to the series relation between the shaft segments and the contact interface in the structure, the flexural stiffness of the rod-fastened Jeffcott rotor can be expressed as

$$K_s = \frac{2L_1 + L_2}{((2L_1/EI_1) + (L_2/EI_2) + (1/G_r))}, \quad (1)$$

where G_r is the equivalent flexural stiffness of the contact interface and E is the elastic modulus of the material.

According to the statistical model of rough surface contact proposed by Greenwood and Williamson, the contact of the two rough surfaces is the contact behavior of the microconvex bodies distributed on them. The relationship of the pressure between the contact surfaces and the distance between the two reference surfaces of the rough contact surface [21] can be written as

$$P = \frac{4}{3\sigma\sqrt{2\pi}}\eta A_{\text{nom}}E'\beta^{1/2} \int_d^{\infty} (z - d_0)^{3/2} e^{-(z^2/2\sigma^2)} dz, \quad (2)$$

where P is the pressure between the contact surfaces and is the root mean square of the height distribution of the microconvex body. η is the distribution density of the microconvex body of the rough contact surface. β is the average radius of curvature of the top of the microconvex body. E' is the equivalent elastic modulus of the material. A_{nom} is the nominal contact area of the contact interface. d_0 is the distance between two reference contact planes without relative rotation after the preload is applied. z is the height parameter of the microconvex body.

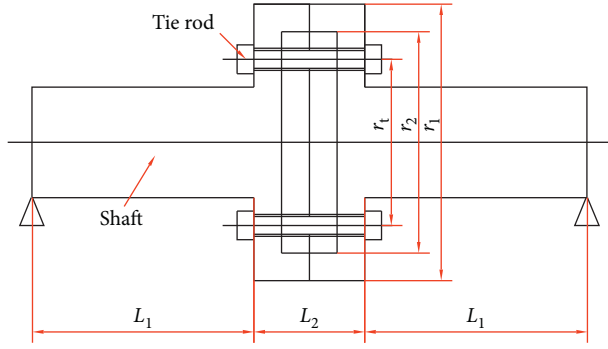


FIGURE 1: The rod-fastened Jeffcott rotor.

The equivalent flexural stiffness of the contact interface [21] can be written as

$$G_r = \frac{\partial M}{\partial \theta}$$

$$= -\frac{2}{\sigma\sqrt{2\pi}} \eta E' \beta^{1/2} \int_{A_{\text{nom}}} \int_{d_0}^{\infty} (z - d_0 - y\theta)^{3/2} e^{-(z^2/2\sigma^2)} y^2 dz dA_{\text{nom}}, \quad (3)$$

where G_r is the equivalent flexural stiffness of the contact interface. M is the bending moment applied to the contact interface. y is the radial parameter of the contact surface. θ is the rotation angle between two contact planes.

$$G_{ry} = -\frac{2}{\sigma\sqrt{2\pi}} \eta E' \beta^{1/2} \int_{-(\pi/8)}^{\pi/8} d\varphi \int_{r_1}^{r_2} r dr \int_{d_1}^{\infty} (z - d_1 - r\theta \sin \varphi)^{3/2} e^{-(z^2/2\sigma^2)} \cdot r^2 \sin^2 \varphi dz$$

$$- \frac{2}{\sigma\sqrt{2\pi}} \eta E' \beta^{1/2} \int_{\pi/8}^{2\pi-(\pi/8)} d\varphi \int_{r_1}^{r_2} r dr \int_{d_1}^{\infty} (z - d_0 - r\theta \sin \varphi)^{3/2} e^{-(z^2/2\sigma^2)} \cdot r^2 \sin^2 \varphi dz, \quad (5)$$

$$G_{rx} = -\frac{2}{\sigma\sqrt{2\pi}} \eta E' \beta^{1/2} \int_{-(\pi/8)}^{\pi/8} d\varphi \int_{r_1}^{r_2} r dr \int_{d_1}^{\infty} (z - d_1 - r\theta \cos \varphi)^{3/2} e^{-(z^2/2\sigma^2)} \cdot r^2 \cos^2 \varphi dz$$

$$- \frac{2}{\sigma\sqrt{2\pi}} \eta E' \beta^{1/2} \int_{\pi/8}^{2\pi-(\pi/8)} d\varphi \int_{r_1}^{r_2} r dr \int_{d_1}^{\infty} (z - d_0 - r\theta \cos \varphi)^{3/2} e^{-(z^2/2\sigma^2)} \cdot r^2 \cos^2 \varphi dz,$$

where r and φ are the polar coordinate parameters.

Due to the detuning of the clamping force of the tie rods, the equivalent flexural stiffness of the contact interface along the x -direction and y -direction will be not equal, which will lead to the rod-fastened Jeffcott rotor with asymmetric flexural stiffness along with the two main stiffness directions.

2.2. The Equation of Motion of the Rod-Fastened Jeffcott Rotor. According to Euler-Bernoulli theory, the lateral stiffness of the rod-fastened Jeffcott rotor can be given by

$$K_{ji} = 48K_{si}(2L_1 + L_2)^{-3} = 48 \left(\frac{2L_1}{EI_1} + \frac{L_2}{EI_2} + \frac{1}{G_{ri}} \right)^{-1} (2L_1 + L_2)^{-2}, \quad (6)$$

The contact surface and the distribution of tie rods can be seen in Figure 2. Corresponding to eight tie rods, the annular contact interface is equally divided into eight parts, from S1 to S8. When the clamping force of each tie rod is equal, the contact stress on the whole contact surface is uniform. However, when the clamping force of one tie rod is different from the other tie rods, the detuning of the clamping force between the tie rods have occurred. When the clamping force of the detuning tie rod is f_d and the clamping force of the other tuning tie rods are f_t , the detuning rate of the clamping force of one tie rod can be written as

$$D = \frac{f_d - f_t}{f_t}. \quad (4)$$

When D is greater than zero, it means the positive detuning of the tie rod. When D is less than zero, it means the negative detuning of the tie rod. If one tie rod is out of tune, in the detuning part of the contact interface, the distance between reference planes of the two rough contact surfaces d_1 will be different from the distance d_0 under the tuning condition (see Figure 3).

For example, in Figure 2, when only the No. 1 tie rod is out of tune, the equivalent flexural stiffness of the contact interface along the x -direction and y -direction can be written as

where $i = x, y$. The x -direction and y -direction respect two main stiffness directions.

Figure 4 is the sketch map of the motion of the Jeffcott rotor. In Figure 4, O_d is denoted as the geometry center of the disc, and O_g is denoted as the center of mass. δ_r is the residual shaft bow, e is the eccentricity, ω is the angular velocity of the rotor, and Ψ_0 is the initial phase angle of the eccentric. Z is the dynamic displacement of the geometry center of the disc, and Z_g is the dynamic displacement of the center of mass of the rotor. xoy is the static coordinate system, and $\xi o\eta$ is the dynamic coordinate system. Because the flexural stiffness of the rotor along the x -direction and y -direction is not equal, it is necessary to express the equation of motion of the rod-fastened Jeffcott rotor in the dynamic coordinate system. In the xoy coordinate system, the equation of motion of the rod-fastened Jeffcott rotor can be written as

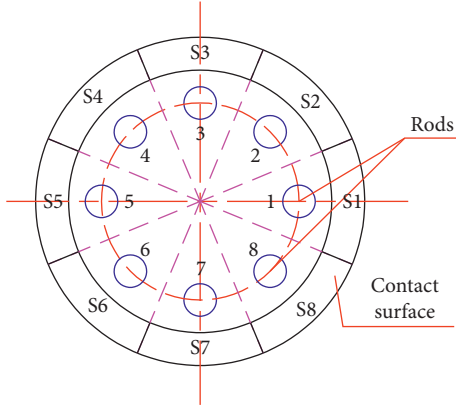


FIGURE 2: The contact surface and the distribution of tie rods.

$$\begin{bmatrix} m & \\ & m \end{bmatrix} \begin{bmatrix} \ddot{x}_g & \ddot{y}_g \end{bmatrix} + \begin{bmatrix} k_x & 0 \\ 0 & k_y \end{bmatrix} \begin{bmatrix} x \\ y \end{bmatrix} = 0. \quad (7)$$

$$\begin{bmatrix} \cos(\omega t) & -\sin(\omega t) \\ \sin(\omega t) & \cos(\omega t) \end{bmatrix} \begin{bmatrix} \ddot{\xi} \\ \ddot{\eta} \end{bmatrix} + 2\omega \begin{bmatrix} -\sin(\omega t) & -\cos(\omega t) \\ \cos(\omega t) & -\sin(\omega t) \end{bmatrix} \begin{bmatrix} \dot{\xi} \\ \dot{\eta} \end{bmatrix} + \begin{bmatrix} \omega_{k1}^2 - \omega^2 & 0 \\ 0 & \omega_{k2} - \omega^2 \end{bmatrix} \begin{bmatrix} \cos(\omega t) & -\sin(\omega t) \\ \sin(\omega t) & \cos(\omega t) \end{bmatrix} \begin{bmatrix} \xi \\ \eta \end{bmatrix} = \omega^2 \begin{bmatrix} \cos(\omega t) & -\sin(\omega t) \\ \sin(\omega t) & \cos(\omega t) \end{bmatrix} \begin{bmatrix} \xi_0 \\ \eta_0 \end{bmatrix} + e\omega^2 \begin{bmatrix} \cos \psi_0 \\ \sin \psi_0 \end{bmatrix}, \quad (8)$$

where ξ_0 and η_0 are the residual shaft bow deformation in the $\xi\eta$ coordinate system. $\omega_{k1} = \sqrt{k_x/m}$ and $\omega_{k2} = \sqrt{k_y/m}$ are the two first-order natural frequencies. In the rotating coordinate system, ξ, η , and η take two main stiffness directions. Thus, $k_\xi = K_{Jx}$ and $k_\eta = K_{Jy}$.

When there is no eccentric of the mass of the rotor, the amplitude of steady response of the rod-fastened Jeffcott rotor with residual shaft bow can be derived from Equation 8. It can be given by

$$A_r = \begin{bmatrix} \frac{\omega^2 \xi_0}{|\omega_{k1}^2 - \omega^2|} \\ \frac{\omega^2 \eta_0}{|\omega_{k2}^2 - \omega^2|} \end{bmatrix}, \quad (9)$$

where ω is the angular speed of the rotor; ω_{k1} and ω_{k2} are the two first-order natural frequencies. A_r takes the maximum value of vibration response in two directions ξ, η .

2.3. The Calculation of the Residual Shaft Bow Deformation. The detuning of the clamping force of the tie rods will lead to the rotor with the residual shaft bow. The residual shaft bow deformation will directly affect the vibration response. Therefore, the accurate calculation of the residual shaft bow deformation is essential.

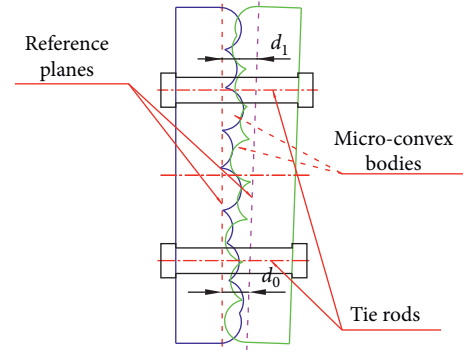


FIGURE 3: The skeptical of the contact interface when the tie rod is out of tune.

It is easy to write the equation of motion of the rod-fastened Jeffcott rotor in the $\xi\eta$ coordinate system. It can be given by

From Figure 5, the clamped shaft segment has certain residual shaft bow deformation due to the detuning of the clamping force of the tie rods. When there is one tie rod out of tune, it is easy to know the bending moment can be given by

$$M = \frac{P D r_t}{n}, \quad (10)$$

where P is the preload of the rotor, r_t is the installation radius of the tie rods, and n is the number of the tie rods. D is the detuning rate of the clamping force of one tie rod.

According to the bow deformation relation, the deflection angle of the rotor axis α can be given by

$$\alpha = \frac{L_2}{2R} = \frac{M}{2} \left(\frac{L_2}{EI_2} + \frac{1}{G_r} \right). \quad (11)$$

Therefore, the residual shaft bow deformation of the rotor can be written as

$$\delta_r = R(1 - \cos \alpha) + L_1 \sin \alpha. \quad (12)$$

Therefore, in the above section, $\xi_0 = \delta_{r1}$ and $\eta_0 = \delta_{r2}$.

3. Results and Discussion

3.1. The Rotor Model. The rod-fastened Jeffcott rotor is shown in Figure 1. The main physical parameters are listed as follows: $L_1 = 0.2$ m and $L_2 = 0.1$ m. The outer radius of the

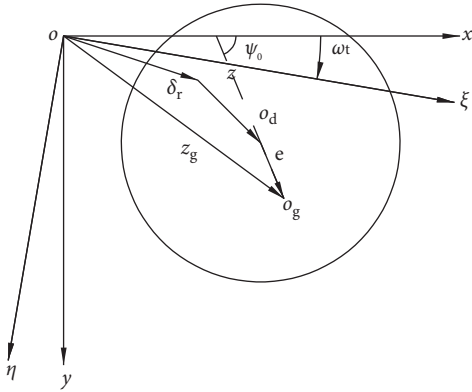


FIGURE 4: The sketch map of the motion of the Jeffcott rotor.

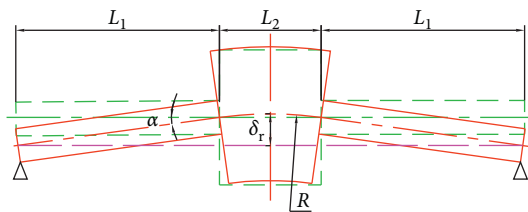


FIGURE 5: The residual shaft bow of the rod-fastened Jeffcott rotor resulted from the detuning of the clamping force of the tie rods.

contact annulus $r_1 = 0.125$ m, and the inner radius of the contact annulus $r_2 = 0.1$ m. The installation radius of the tie rods $r_t = 0.075$ m. The elastic modulus of the material is $E = 1.99e11$ N/m². The density of the material is $\rho = 7.85e3$ kg/m³. The mass of the rotor is $m = 50.84$ kg. The number of the tie rods is $n = 8$.

The detuning of the clamping force of the tie rod will affect the frequency and the residual shaft bow response of the rod-fastened Jeffcott rotor. The following paper is mainly to investigate the effect law of the preload, the rate of detuning of tie rods, and the number of the detuning tie rods on the dynamic performance of the rod-fastened Jeffcott rotor.

3.2. The Effect of the Preload. According to the reference papers mentioned above, the preload is crucial to the rod-fastened rotor. It directly affects the contact state of the contact interface between the discs, which in turn affect the dynamic performance of the rotor system. As shown in Figure 6, the frequency of the rod-fastened Jeffcott rotor is monotonously increasing with the increase of preload. When the preload is larger than 5e4N, the rate of increase of the frequency of the rod-fastened Jeffcott rotor is very slow. That is, because in this situation, the frequency of the rod-fastened Jeffcott rotor is almost very close to the frequency of the corresponding integral rotor. That is to say, when the preload is relatively small, the contact state of the contact interface has a greater influence on the dynamic performance of the rod-fastened rotor.

Figures 7 and 8 plot the effect of the preload on the frequency of the rotor system when one tie rod is out of tune. In the figures, rf1, rf2 respects the rate of change of two natural frequencies. rf1, rf2 can be given by

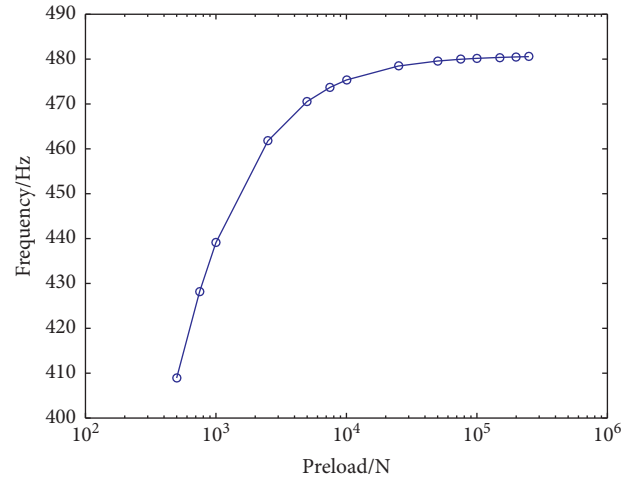


FIGURE 6: The change of the frequency of the rod-fastened Jeffcott rotor with the preload.

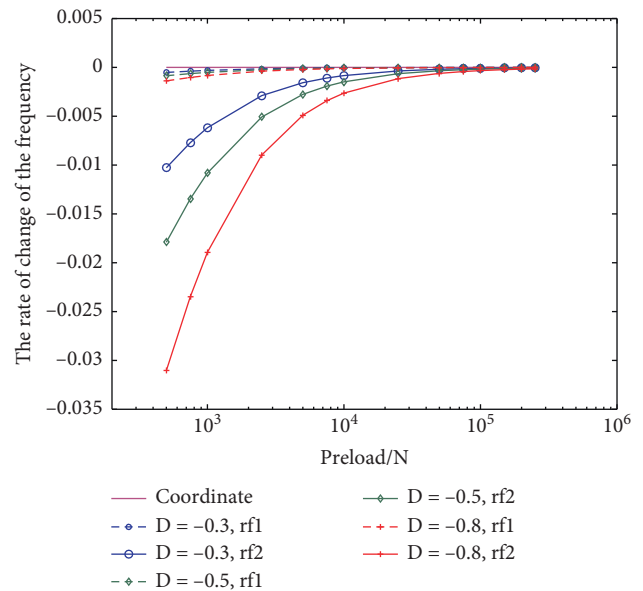


FIGURE 7: The rate of change of the frequency of the rotor with preload when one tie rod has a negative detuning.

$$rfi = \frac{F_{di} - F_t}{F_t} \quad i = 1, 2, \quad (13)$$

where F_t is the natural frequency of the rotor system when the clamping force of the tie rods is uniform, while F_d is the natural frequency of the rotor system when the clamping force of the tie rods is detuning.

It shows that the detuning of the tie rods leads to the flexural stiffness of the rod-fastened is not equal along the two main stiffness directions, which makes the rotor have two first-order frequencies. The negative detuning of the tie rod makes the frequency of the rotor decrease, while the positive detuning of the tie rod makes the frequency of the rotor increase. The absolute value of the rate of change of the frequency of the rotor is decreasing with the increase of preload. It means that the detuning of the tie rod has a

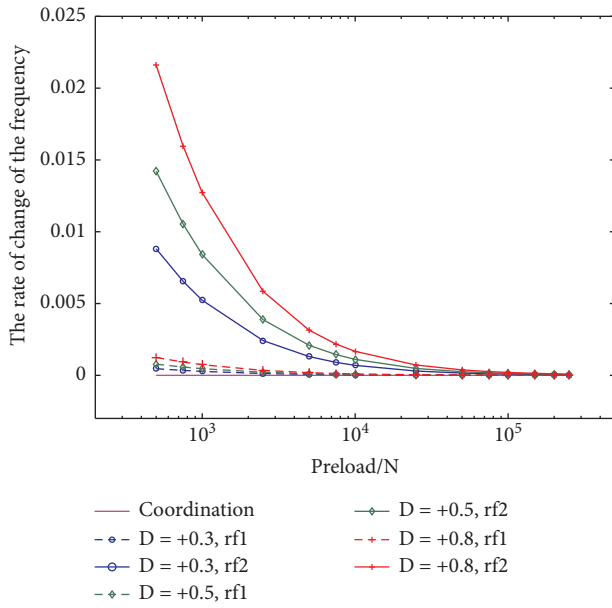


FIGURE 8: The rate of change of the frequency of the rotor with preload when one tie rod has a positive detuning.

greater effect on the frequency of the rotor when the preload is relatively smaller. When the preload is larger than $5e4N$, the effect of detuning of one tie rod on the frequency of the rotor is very small and almost negligible. When the preload is the same, the larger absolute value of the rate of detuning of the tie rod has a greater influence on the frequency of the rotor. Comparing Figure 7 with Figure 8, under the same preload and the absolute value of the rate of detuning of the tie rod, the negative detuning of the tie rod has a large effect than the positive detuning of the tie rod.

Figure 9 plots the effect of the preload on the residual shaft bow deformation of the rotor system and the effect of the preload on the response amplitude of the rotor with a certain speed (2407 rad/s) when one tie rod has a negative detuning. It shows that the residual shaft bow deformation is monotonously increasing with the increase of the preload. However, the amplitude of response of the rotor with a certain speed decreases firstly and then increases with the increase of the preload. The preload of the trend turning point is about $2.5e3N$. This is because, when the preload is smaller than $2.5e3N$, the flexural stiffness of the rod-fastened rotor is relatively smaller. Although the residual shaft bow deformation of the rotor is small, the response amplitude of the rotor is not very small. In this situation, the flexural stiffness of the rod-fastened rotor is the deciding factor. The flexural stiffness of the rod-fastened rotor is increasing with the increase of the preload and the amplitude of response of the rotor decreases. When the preload is larger than $2.5e3N$, the flexural stiffness of the rod-fastened rotor is relatively larger, and the rate of change of the flexural stiffness of the rod-fastened rotor is relatively smaller. In this situation, the residual shaft bow deformation of the rod-fastened rotor is the deciding factor. The residual shaft bow deformation of the rotor is increasing rapidly with the increase of the preload, and the response amplitude of the rotor also

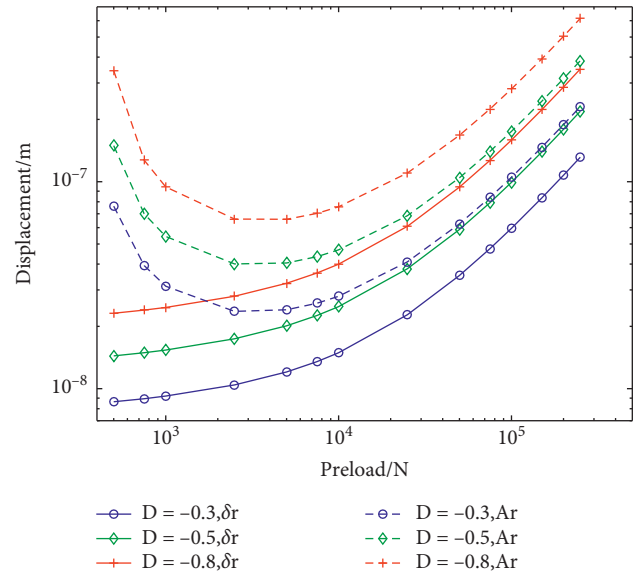


FIGURE 9: The change of the residual shaft bow deformation and the response amplitude of the rotor with preload when one tie rod has a negative detuning.

increases rapidly. The larger absolute value of the rate of detuning of the tie rod has a greater influence on the residual shaft bow deformation and the response amplitude of the rotor.

Figure 10 plots a comparison of the residual shaft bow deformation and the response amplitude of the rotor under the conditions of the positive detuning and the negative detuning of one tie rod. It is shown that the effect law of the positive detuning of the tie rods and the negative detuning of the tie rods on the residual shaft bow deformation and the response amplitude of the rotor are the same. However, the negative detuning of the tie rods has a larger residual shaft bow deformation and the response amplitude of the rotor compared with the positive detuning of the tie rods at the same preload and absolute value of the rate of detuning of the tie rod, especially when the preload is relatively smaller.

3.3. The Effect of the Rate of Detuning of Tie Rods.

Figures 11 and 12 plot the effect of the rate of detuning of one tie rod on the frequency of the rotor. It can be seen that the negative detuning of the tie rod and the negative detuning of the tie rod all make the absolute value of the rate of change of the frequency of the rotor increase with the increase of the rate of detuning of one tie rod. It means that the larger the rate of detuning of tie rods have a greater influence on the frequency of the rotor. Under different preload situations, the effect law of the rate of detuning of tie rods on the frequency of the rotor is the same. When the rate of detuning of the tie rod is the same, the smaller preload has a greater influence on the frequency of the rotor.

Figure 13 plots the effect of the rate of negative detuning of one tie rod on the residual shaft bow deformation of the rotor system and the effect of the rate of negative detuning of one tie

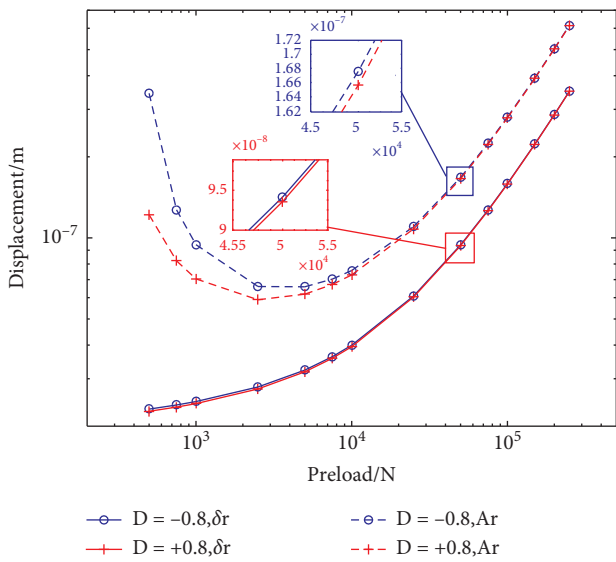


FIGURE 10: A comparison of the residual shaft bow deformation and the response amplitude of the rotor under the conditions of the positive detuning and the negative detuning of one tie rod.

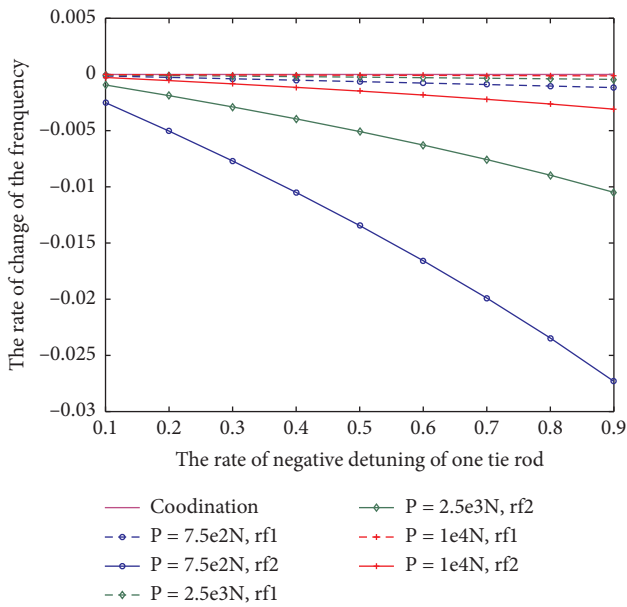


FIGURE 11: The rate of change of the frequency of the rotor with the rate of negative detuning of one tie rod.

rod on the amplitude of response of the rotor with a certain speed. It shows that the residual shaft bow deformation is linear monotonously increasing with the increase of the absolute value of the rate of negative detuning of one tie rod. The response amplitude of the rotor with a certain speed also increases with the increase of the preload. When the preload is smaller, the amplitude of response of the rotor increases exponentially with the increase of the preload, and the speed of increase is faster. When the preload is larger than 2.5e3N, the increase of the response amplitude of the rotor is linear.

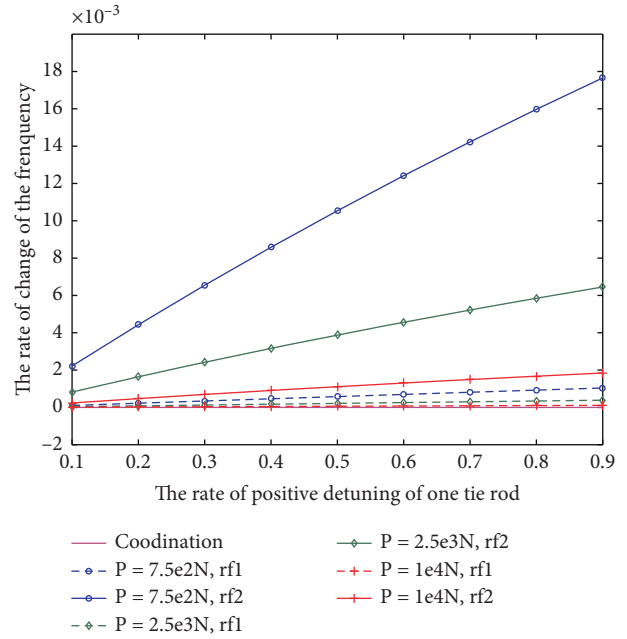


FIGURE 12: The rate of change of the frequency of the rotor with the rate of positive detuning of one tie rod.

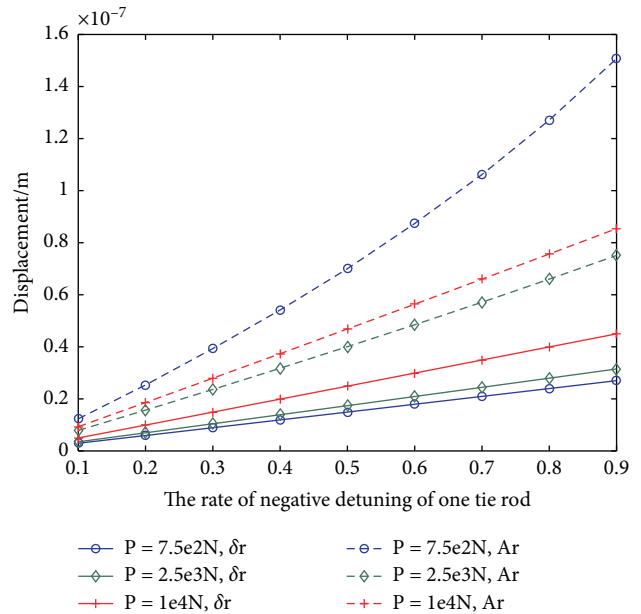


FIGURE 13: The change of the residual shaft bow deformation and the response amplitude of the rotor with the rate of negative detuning of one tie rod.

Figure 14 plots a comparison of the change of the residual shaft bow deformation and the response amplitude of the rotor with the absolute value of the rate of detuning of one tie rod under the conditions of the positive detuning and the negative detuning of one tie rod. It is shown that the change of the residual shaft bow deformation and the response amplitude of the rotor with the absolute value of the rate of detuning of one tie rod is the same under the positive

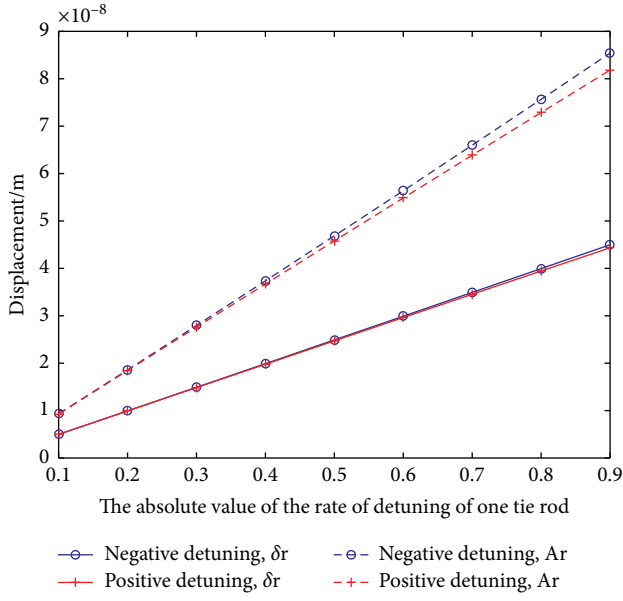


FIGURE 14: A comparison of the residual shaft bow deformation and the response amplitude of the rotor under the conditions of the positive detuning and the negative detuning of one tie rod.

detuning of the tie rods and the negative detuning of the tie rods. The negative detuning of the tie rods have a larger residual shaft bow deformation and the response amplitude of the rotor compared with the positive detuning of the tie rods when the preload is relatively larger.

3.4. The Effect of the Number of the Detuning Tie Rods. Figure 15 plots the rate of change of the frequency of the rotor with the preload under the different numbers of detuning tie rods. The rate of detuning of the tie rods is -0.5 . It shows that, under different numbers of detuning tie rods, the change law of the rate of change the frequency of the rotor with the increase of preload is similar. However, the larger number of detuning tie rods have a greater influence on the frequency of the rotor. Especially, when the preload is small, the number of detuning tie rods is four, the rate of change of the frequency of the rotor almost reaches 4.5%. Besides, the larger number of detuning tie rods makes the two frequencies of the rotor closer to each other. It means that the larger number of detuning tie rods makes the flexural stiffness along the two main stiffness direction tend to be consistent. The positive detuning of the tie rods makes the frequency of the rotor increase, and this is just contrary to the result of the negative detuning of the tie rods. But the effect law of the number of detuning tie rods on the frequency of the rotor is absolutely consistent.

Figure 16 plots the rate of change of the frequency of the rotor with the rate of detuning of the tie rods under the different numbers of detuning tie rods. The preload of the rotor is $2.5e3N$. As seen from Figure 16, under different numbers of detuning tie rods, the change law of the rate of change of the frequency of the rotor is similar. The larger number of detuning tie rods have a greater influence on the frequency of the rotor. When the rate of detuning of the tie

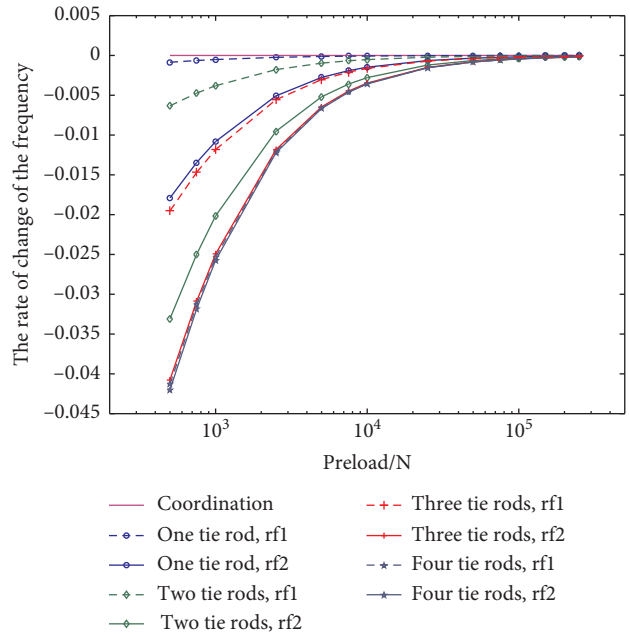


FIGURE 15: The rate of change of the frequency of the rotor with the preload under the different number of detuning tie rods.

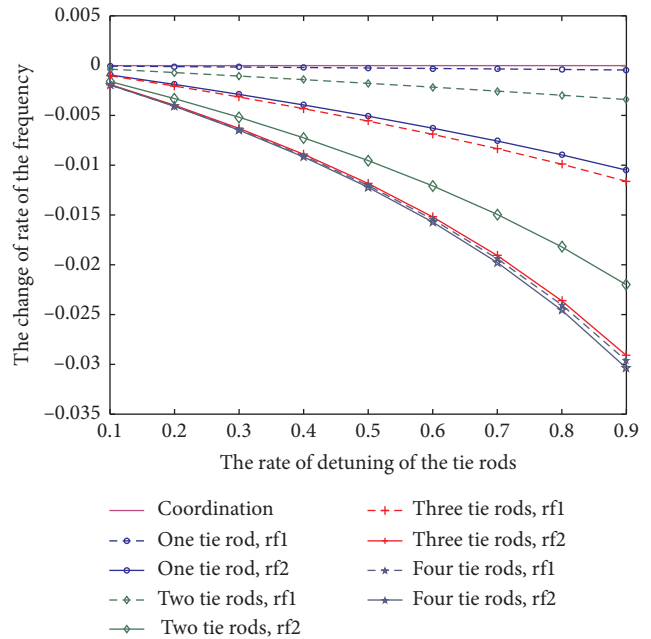


FIGURE 16: The rate of change of the frequency of the rotor with the rate of detuning of the tie rods under different number of detuning tie rods.

rods is larger, the number of detuning tie rods has a greater influence on the frequency of the rotor.

Figure 17 plots the change of the residual shaft bow deformation and the response amplitude of the rotor with the preload under different numbers of detuning tie rods. The rate of detuning of the tie rods is -0.5 . It shows that the effect law of the preload on the residual shaft bow

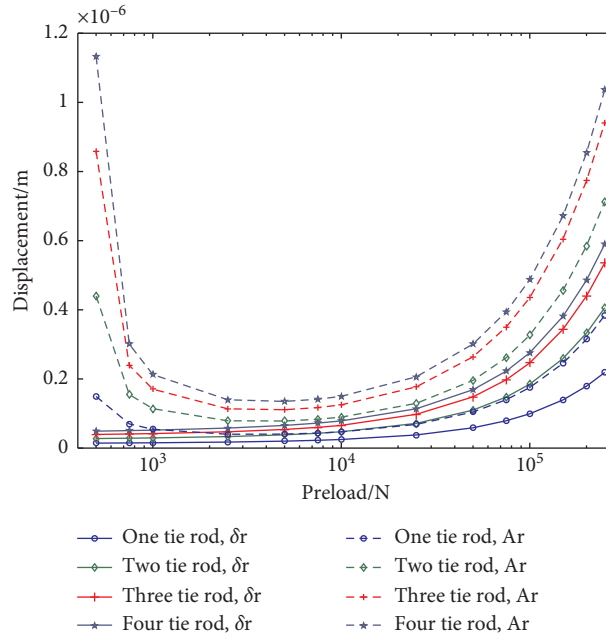


FIGURE 17: The change of the residual shaft bow deformation and the response amplitude of the rotor with the preload under different number of detuning tie rods.

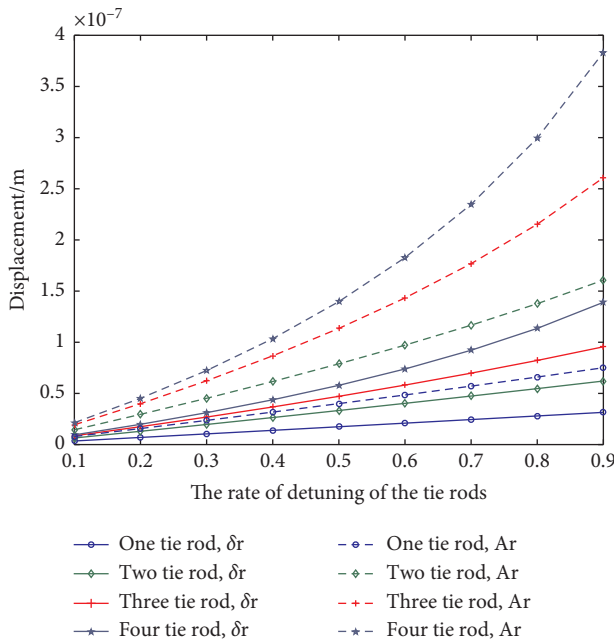


FIGURE 18: The change of the residual shaft bow deformation and the response amplitude of the rotor with the rate of negative detuning of the tie rods under different number of detuning tie rods.

deformation and the amplitude of response of the rotor under the different number of detuning tie rods is consistent. The larger number of detuning tie rods makes the rotor have a greater residual shaft bow deformation, which leads to a greater amplitude of response of the rotor.

Figure 18 plots the change of the residual shaft bow deformation and the amplitude of response of the rotor with

the rate of negative detuning of the tie rods under the different number of detuning tie rods. The preload of the rotor is $2.5e3N$. It shows that, when the rate of detuning of the tie rods is larger, the larger number of detuning tie rods has a greater influence on the frequency of the rotor.

4. Summary and Conclusions

Based on the GW contact model, this study presents a new method to calculate the equivalent flexural stiffness of rough surface considering the detuning of clamping force of the tie rods and gives the calculation method of the residual shaft bow deformation of the rod-fastened Jeffcott rotor with detuning of the tie rods. The effect of the preload, the rate of detuning of the tie rods, and the number of detuning tie rods on the dynamic performance of the rod-fastened Jeffcott rotor are investigated. Some conclusions can be drawn as follows:

- (1) The detuning of the tie rods makes the flexural stiffness of the rotor inconsistent along the two main stiffness directions of the rotor, which makes the natural frequency of the rotor divided into two.
- (2) The negative detuning of the tie rods decreases the natural frequency of the rotor, while the positive detuning of the tie rods increases the natural frequency of the rotor. The smaller preload or the larger rate of detuning of the tie rods make the detuning of the tie rods have a greater influence on the natural frequency of the rotor.
- (3) With the increase of the preload, the residual shaft bow deformation of the rotor increases monotonically due to the detuning of the tie rods, and the response amplitude of the residual shaft bow of the

rotor decreases firstly and then increases. This is because, when the preload is relatively smaller, the flexural stiffness of the rod-fastened rotor is also relatively smaller. At this time, although the residual shaft bow deformation of the rotor is small, the amplitude of response of the rotor is not very small, because the flexural stiffness of the rod-fastened rotor is the deciding factor at present. The flexural stiffness of the rod-fastened rotor is increasing with the increase of the preload, and the amplitude of response of the rotor decreases. When the preload is relatively larger, the flexural stiffness of the rod-fastened rotor is also relatively larger, and the rate of change of the flexural stiffness of the rod-fastened rotor is relatively smaller. In this situation, the residual shaft bow deformation of the rod-fastened rotor is the deciding factor. The residual shaft bow deformation of the rotor is increasing rapidly with the increase of the preload, and the response amplitude of the rotor also increases rapidly.

- (4) With the increase of the rate of detuning of the tie rods, the residual shaft bow deformation and response amplitude of the rotor all increase monotonically. Compared with the positive detuning of the tie rods, the negative detuning of the tie rods has a greater impact on the natural frequency of the rotor and makes the response amplitude of the rotor larger. The more number of detuning tie rods has the greater influence on the natural frequency and response amplitude of the rotor.

Data Availability

The data used to support the findings of this study are included within the article.

Conflicts of Interest

The authors declare that they have no conflicts of interest.

Acknowledgments

The authors would like to express their sincere gratitude to the National Natural Science Foundation of China (Grant nos. 11872288 and 51575425), Shaanxi Provincial Natural Science Foundation of China (Grant no. 2019JM-219), and the National High-tech Research and Development Program of China (Grant no. 2013CB035706).

References

- [1] Z. S. Rao, "A study of dynamic characteristic and contact stiffness of the rod fastening composite special rotor," Ph.D. Dissertation, Harbin Institute of Technology, Harbin, China, 1992.
- [2] Q. Yuan, R. Gao, Z. Feng, and J. Wang, "Analysis of dynamic characteristics of gas turbine rotor considering contact effects and pre-tightening force," in *Proceedings of the ASME Turbo Expo 2008: Power for Land, Sea, and Air. Volume 5: Structures and Dynamics, Parts A and B*, Berlin, Germany, June 2008.
- [3] Y. C. Zhang, Z. Du, L. Shi, and S. Liu, "Determination of contact stiffness of rod-fastened rotors based on modal test and finite element analysis," *Journal of Engineering for Gas Turbines and Power*, vol. 132, no. 9, 2010.
- [4] J. E. Jam, F. Meisami, and N. G. Nia, "Vibration analysis of tie-rod/tie-bolt rotors using FEM," *International Journal of Engineering Science and Technology*, vol. 3, no. 10, pp. 7292–7300, 2011.
- [5] P. He, Z. Liu, and G. Zhang, "A study of overall contact behavior of an elastic perfectly plastic hemisphere and a rigid plane," *Proceedings of the Institution of Mechanical Engineers, Part J: Journal of Engineering Tribology*, vol. 227, no. 3, pp. 259–274, 2012.
- [6] P. He, Z. Liu, F. Huang, and R. Ma, "A study of elastic-plastic contact of statistical rough surfaces," *ARCHIVE Proceedings of the Institution of Mechanical Engineers Part J Journal of Engineering Tribology 1994-1996*, vol. 227, no. 10, pp. 1076–1089, 2013.
- [7] H. Peng, Z. Liu, G. Wang, and M. Zhang, "Rotor dynamic analysis of tie-bolt fastened rotor based on elastic-plastic contact," in *Proceedings of ASME Turbo Expo: Turbine Technical Conference and Exposition*, Vancouver, British Columbia, Canada, June 2011.
- [8] M. J. Lu, H. Geng, B. Yang, and L. Yu, "Finite element method for disc-rotor dynamic characteristics analysis of gas turbine rotor considering contact effects and rod preload," in *Proceedings of the 2010 IEEE International Conference on Mechatronics and Automation*, Xi'an, China, August 2010.
- [9] J. Gao, Q. Yuan, P. Li, Z. Feng, H. Zhang, and Z. Lv, "Effects of bending moments and pre-tightening forces on the flexural stiffness of contact interfaces in rod-fastened rotors," *Journal of Engineering for Gas Turbines and Power*, vol. 134, no. 10, 8 pages, 2012.
- [10] H. Liu, L. Chen, W. Wang, X. Qi, and M. Jing, "Nonlinear dynamic analysis of a flexible rod fastening rotor-bearing system," in *Proceedings of ASME Turbo Expo 2010: Power for Land, Sea, and Air*, Glasgow, UK, June 2010.
- [11] J. Yi, H. Liu, Y. Liu, and M. Jing, "Global nonlinear dynamic characteristics of rod-fastened rotor supported by ball bearings," *Proceedings of the Institution of Mechanical Engineers Part K Journal of Multi-body Dynamics*, vol. 229, no. 2, pp. 208–222, 2014.
- [12] Q. Yuan, J. Gao, and P. Li, "Nonlinear dynamics of the rod-fastened Jeffcott rotor," *Journal of Vibration and Acoustics*, vol. 136, no. 2, pp. 1–10, 2014.
- [13] L. Hu, Y. Liu, L. Zhao, and C. Zhou, "Nonlinear dynamic behaviors of circumferential rod fastening rotor under unbalanced pre-tightening force," *Archive of Applied Mechanics*, vol. 86, no. 9, pp. 1621–1631, 2016.
- [14] J. C. Nicholas, E. J. Gunter, and P. E. Allaire, "Effect of residual shaft bow on unbalance response and balancing of a single mass flexible rotor-part I: unbalance response," *Journal of Engineering for Power*, vol. 98, no. 2, pp. 171–181, 1976.
- [15] R. D. Flack and J. H. Rooke, "A theoretical-experimental comparison of the synchronous response of a bowed rotor in five different sets of fluid film bearings," *Journal of Sound and Vibration*, vol. 73, no. 4, pp. 505–517, 1980.
- [16] T. N. Shiau and E. K. Lee, "The residual shaft bow effect on the dynamic response of a simply supported rotor with disk skew and mass unbalances," *Journal of Vibration, Acoustics, Stress, and Reliability in Design*, vol. 111, no. 2, pp. 170–178, 1989.
- [17] J. S. Rao, "A note on Jeffcott warped rotor," *Mechanism and Machine Theory*, vol. 36, no. 5, pp. 563–575, 2001.

- [18] C. H. Kang, W. C. Hsu, E. K. Lee, and T. N. Shiau, "Dynamic analysis of gear-rotor system with viscoelastic supports under residual shaft bow effect," *Mechanism and Machine Theory*, vol. 46, no. 3, pp. 264–275, 2011.
- [19] G. F. Song, Z. J. Yang, C. Ji, and F. P. Wang, "Theoretical-experimental study on a rotor with a residual shaft bow," *Mechanism and Machine Theory*, vol. 63, pp. 50–58, 2013.
- [20] F. D. Sanches and R. Pederiva, "Theoretical and experimental identification of the simultaneous occurrence of unbalance and shaft bow in a Laval rotor," *Mechanism and Machine Theory*, vol. 101, pp. 209–221, 2016.
- [21] P. He, "Analysis of dynamic characteristics of distributed rod fastening rotor," Master Dissertation, Harbin Institute of Technology, Harbin, China, 2009.